

Kerkes, D. J., "**Analysis and Prediction of Stresses and Pore Pressures Associated with Wet Core Construction for Embankment Dams**," a thesis submitted to the faculty of the Graduate School of the University of Colorado in partial fulfillment of the requirements for the degree of Doctor of Philosophy, May 1990

Thesis directed by Professor Robert L. Schiffman

ABSTRACT

The wet core construction method has been successfully applied to embankment dams in parts of the world that experience high annual rainfall, where the natural moisture content of core zone construction material is so far above optimum as to render fill placement to conventionally accepted standards infeasible. While the method has definite advantages in terms of construction cost and schedule, a significant disadvantage is associated with the high pore pressures that develop during construction. This study examines the factors governing pore pressure generation, as well as those affecting the distribution of stresses within the embankment. The primary purpose of the investigation was to develop a simple analytical model that could be used for routine design purposes to estimate the pore pressures that develop during construction in the core of a zoned embankment. Field data from a 394 feet (120 meter) high wet core dam constructed in Indonesia was used to validate the model. The secondary objective was to study the instrumentation data obtained from total stress cells, piezometers and settlement devices, in an effort to better understand the internal stress distribution, pore pressures and consolidation that occur in a zoned embankment with a wet core.

The investigation yielded a relatively straightforward analytical model for estimating pore pressures in the core of a zoned embankment that can be executed using a desk top personal computer and commercially available spreadsheet software. The primary components of the model consist of (1) an approximate method for estimating the stresses within the core, (2) an algorithm for computing the pore pressures generated in the core, which considers the effect of partial saturation, and (3) a two-dimensional finite difference solution for the uncoupled multi-dimensional consolidation theory of Terzaghi-Rendulic to account for pore pressure dissipation during construction. The model can be adapted to virtually any core zone geometry, simulates the advancing fill by providing for a moving upper boundary that can be controlled to approximate the actual construction sequence, and permits pore pressures along the upstream boundary to be varied to model reservoir impoundment. The solution algorithms for the model are presented in detail.

CONTENTS

CHAPTER

I.	INTRODUCTION	1
II.	ZONED EMBANKMENT DAM DESIGN CONCEPTS	10
III.	PREVIOUS INVESTIGATIONS	24
IV.	WADASLINTANG DAM	31
	Project Description	31
	Site Geology	31
	Climate	33
	Core Material	33
	Core Placement	36
	Instrumentation	37
V.	PORE PRESSURE RESPONSE IN SOIL	43
	One-Dimensional Compression	43
	Partially Saturated Soil	45
	Pore Pressure Coefficients.	47
	The Cam-Clay Model	49
VI.	INTERNAL STRESS DISTRIBUTION	54
VII.	THE CONSOLIDATION EQUATION AND FINITE DIFFERENCE APPROXIMATION	81
VIII.	THE SPREADSHEET ALGORITHMS	90
IX.	RESULTS OF ANALYSES TO PREDICT PORE PRESSURES	103
X.	SETTLEMENT AND CONSOLIDATION	119
	Settlement Data	119
	Pore Pressure Data	124
XI.	CONCLUSIONS AND RECOMMENDATIONS FOR FURTHER INVESTIGATIONS	132
	BIBLIOGRAPHY	139

APPENDIX

A.	CORE ZONE TOTAL STRESS CELL DATA	148
B.	CORE ZONE PIEZOMETER DATA	154
C.	CORE ZONE SETTLEMENT DATA	160
D.	DETAILS OF THE BASIC SPREADSHEET LAYOUT, MACROS AND FORMULAS	168
E.	DETAILS OF THE CAM-CLAY SPREADSHEET ALGORITHM	178
F.	CONSOLIDATION TEST RESULTS AND CAM-CLAY DATA	186

TABLES

Table

4.1	Core Material Index Properties	35
4.2	Core Zone Quality Control Test Results	36
4.3	Core Zone Instrument Locations	39
10.1	Settlement Data for Sta. 0+465 (Maximum Section)	122
10.2	Steady State and End of Construction Pore Pressures at Selected Piezometers	130
F.1	One-Dimensional Consolidation Test Data Summary	189

FIGURES

Figure

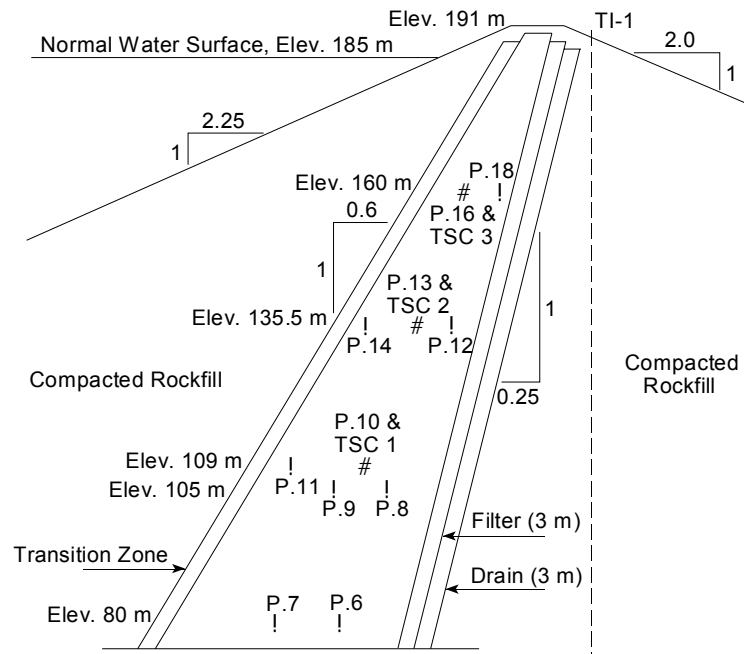
4.1	Typical embankment section	32
4.2	Location of piezometers and total stress cells at the maximum section (Sta 0+465)	40
5.1	Pore pressure response in a partially saturated soil	46
6.1	Approximation for simple elastic embankment model	55
6.2	Reference system for stresses in a simi-infinite elastic half space	56
6.3	Finite element mesh	59

Figure

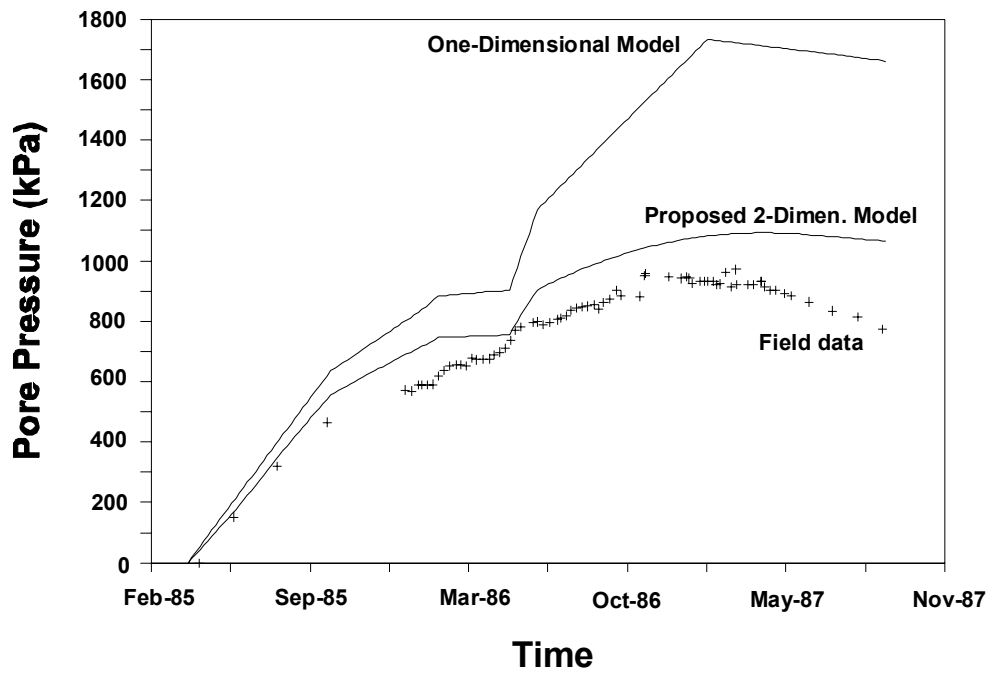
6.4	Reference points for the homogeneous embankment analysis	60
6.5	Total stress in a homogeneous embankment at Point A	62
6.6	Total stress in a homogeneous embankment at Point B	62
6.7	Total stress in a homogeneous embankment at Point C	63
6.8	Total stress in a homogeneous embankment at Point D	63
6.9	Total stress in a homogeneous embankment at Point E	64
6.10	Total stress in a homogeneous embankment at Point F	64
6.11a	Total vertical stresses at TSC 1	66
6.11b	Total horizontal stresses at TSC 1	66
6.12a	Total vertical stresses at TSC 2	67
6.12b	Total horizontal stresses at TSC 2	67
6.13a	Total vertical stresses at TSC 3 and TSC 7	68
6.13b	Total horizontal stresses at TSC 3 and TSC 7	68
6.14a	Total vertical stresses at TSC 4 and TSC 8	69
6.14b	Total horizontal stresses at TSC 4 and TSC 8	69
6.15a	Total vertical stresses at TSC 5	70
6.15b	Total horizontal stresses at TSC 5	70
6.16	Instrument position relative to the external slopes	73
6.17	Percent of embankment height vs D/H Ratio	73
6.18	Effective stress ratio vs time at TSC 1	75
6.19	Effective stress ratio vs time at all TSC's	75
6.20	Total stress ratio at total stress cells	76
6.21a	Total vertical stress vs time at TSC 1	79
6.21b	Total horizontal stress vs time at TSC 1	79
6.22a	Total vertical stress vs time at TSC 5	80
6.22b	Total horizontal stress vs time at TSC 5	80
7.1	Reference system for the finite difference grid	83
8.1	Spreadsheet flow diagram	93
8.2	Core zone finite difference grid	94
8.3	Wadaslintang construction sequence at Sta. 0+465	98

Figure

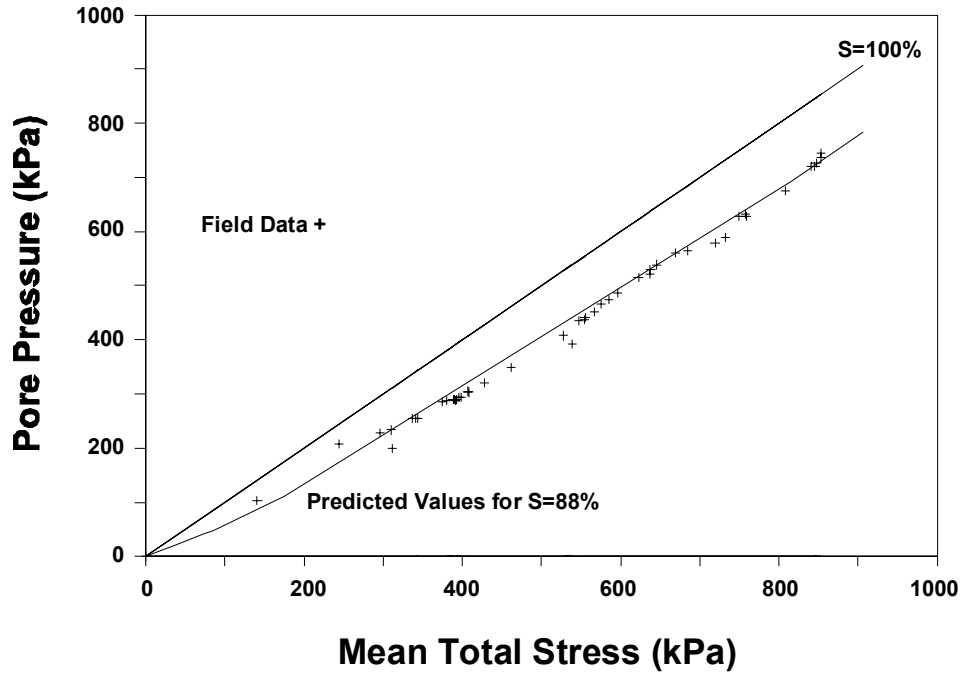
9.1	Pore pressure vs time at P.6	106
9.2	Pore pressure vs time at P.7	106
9.3	Pore pressure vs time at P.8	107
9.4	Pore pressure vs time at P.9	107
9.5	Pore pressure vs time at P.13	108
9.6	Total stress at TSC 1 and pore pressure at P.10	109
9.7	Total stress at TSC 2 and pore pressure at P.13	109
9.8	Total stress at TSC 3 and pore pressure at P.16	110
9.9	Total stress at TSC 5 and pore pressure at P.21	110
9.10	Effect of c_v on pore pressure prediction at P.7	112
9.11	Effect of c_v on pore pressure prediction at P.8	113
9.12	Effect of c_v and the initial partial degree of saturation on the pore pressure prediction at P.6	117
9.13	Effect of c_v and the initial partial degree of saturation on the pore pressure prediction at P.9	117
10.1	Double fluid settlement devices at the maximum section (Sta. 0+465)	121
10.2	Pore pressure response vs mean total stress at TSC 1	125
10.3	Pore pressure response vs mean total stress at TSC 3	126
10.4	Pore pressure response vs mean total stress at TSC 5	126
10.5	End of construction pore pressure distribution at Elev. 80 m (16 Mar 87)	128
10.6	Composite end of construction pore pressure distribution for Elev. 105 and 109 m (13 Apr 87)	128
10.7	End of construction pore pressure distribution at Elev. 135.5 m (10 May 87)	129
D.1	Typical range of nodal values in the spreadsheet	169
D.2	Spreadsheet layout for the basic analysis	171
E.1	Spreadsheet layout for the Cam-Clay model	179
F.1	Volumetric strain vs mean effective stress (p')	188
F.2	Normalized one-dimensional consolidation curve	188



Location of piezometers (P) and total stress cells (TSC) at the maximum section of Wadaslintang Dam. [Fig. 4.2]



Comparison between observed and predicted pore pressures at P.6 [Fig. 9.1]



Pore pressure response vs mean total stress at TSC 1 & P.10 [Fig 10.2 - corrected]
 Predicted values for S=88% developed using Hilf's Method.